Volume 14, Issue 3, Page 130-138, 2025 https://doi.org/10.46810/tdfd.1666413 Research Article

BİNGÖL UNIVERSITY

Türk Doğa ve Fen Dergisi
Turkish Journal of Nature and Science
www.dergipark.gov.tr/tdfd

Synthesis and Characterization of (Sn, Al) Co-doped ZnO Semiconductors

Özlem BİLGİLİ[1*]

[1]Dokuz Eylul University, Science Faculty, Physics Department, Izmir, Turkey
Özlem BİLGİLİ ORCID No: 0000-0002-6334-2513

**Corresponding author: ozlem.bilgili@deu.edu.tr*

(Received: 26.03.2025, Accepted: 10.08.2025, Online Publication: 26.09.2025)

Keywords
Sn and Al co-doped, ZnO, XRD, SEM, EDX, UV-Vis spectroscopy

Abstract: This study presents the effects of tin and aluminium doping and tin/aluminium co-doping on structural, optical, morphological properties of ZnO. Solid state reaction method was used to prepare the samples $Zn_{1-x-y}Sn_xAl_yO$ ((x:y) = (0.00: 0.00), (0.00: 0.03), (0.03: 0.00), (0.03: 0.03)). The properties of the samples were examined by XRD, SEM, EDX spectroscopy and UV–vis spectroscopy. XRD results demonstrated that the lattice parameters a and c, unit cell volume, bond length L decreases while dislocation density increases with doping. The average crystallite size decreased compared to undoped ZnO. SEM images indicated that all samples show presence of hexagonal like grains and grain size decreases with doping. The optical band gaps were estimated from Tauc plots and found as 3.27, 3.26, 3.23, 3.25 eV for undoped and doped $Zn_{0.97}Sn_{0.03}O$, $Zn_{0.97}Al_{0.03}O$ and $Zn_{0.94}Sn_{0.03}Al_{0.03}O$ samples, respectively. The structural and optical calculations showed that characteristic properties of ZnO changed with Al and Sn doping.

(Sn, Al) Eş-katkılı ZnO Yarıiletkenlerinin Sentezi ve Karakterizasyonu

Anahtar Kelimeler
Sn ve Al eş-katkılama, ZnO, XRD, SEM, EDX, UV-Vis spektroskopi

Öz: Bu çalışma, kalay ve alüminyum katkılamasının ve kalay/alüminyum eş katkılamasının ZnO'nun yapısal, optik ve morfolojik özellikleri üzerindeki etkilerini sunmaktadır. Katı hal reaksiyon yöntemi, $Zn_{1-x-y}Sn_xAl_yO$ ((x:y) = (0.00: 0.00), (0.00: 0.03), (0.03: 0.00), (0.03: 0.03)) örneklerini hazırlamak için kullanılmıştır. Örneklerin özellikleri XRD, SEM, EDX spektroskopisi ve UV-vis spektroskopisi ile incelenmiştir. XRD sonuçları, örgü parametreleri a ve c, birim hücre hacmi, bağ uzunluğu L'nin azalırken, dislokasyon yoğunluğunun katkılama ile arttığını göstermiştir. Ortalama kristalit boyutu, katkılanmamış ZnO ile karşılaştırıldığında azalmıştır. SEM görüntüleri, tüm örneklerde hekzagonal benzeri tanelerin varlığını ve tane boyutunun katkılama ile azaldığını göstermiştir. Optik bant aralıkları Tauc grafiklerinden hesaplanmıştır ve sırasıyla katkısız ve katkılı $Zn_{0.97}Sn_{0.03}O$, $Zn_{0.97}Al_{0.03}O$ ve $Zn_{0.94}Sn_{0.03}Al_{0.03}O$ numuneleri için 3.27, 3.26, 3.23, 3.25 eV olarak bulunmuştur. Yapısal ve optik hesaplamalar, ZnO'nun karakteristik özelliklerinin Al ve Sn katkısıyla değiştiğini göstermiştir.

1. INTRODUCTION

Zinc oxide (ZnO) is an II–VI semiconductor with wide direct band gap (3.37 eV) and large exciton binding energy (60 meV) coupled with excellent chemical stability. ZnO is known as an important semiconductor which can be utilized in various areas because of its properties like non-toxicity, being plenty in nature, having low cost, and suitability to doping [1-6].

ZnO doping with transition elements, rare-earth elements, alkaline earth elements, and other elements is extensively worked to reach the desirable optical, electrical, and structural properties [7-20]. The impact of doping by single element on ZnO properties drew significant interest among researchers, and in many studies Al, In, Si, B and Sn were proposed as a good dopant for various metal oxides [21-32]. In addition, numerous studies were deployed to investigate the effects of co-dopant on the optical and structural properties of ZnO [33-44].

The objective of this work is to explore the effects of Al and Sn doping and (Sn–Al) co-doping on the structural and optical properties of ZnO prepared by solid state

reaction method. In this study, the solid-state reaction method was selected due to its advantages, including rapid synthesis, simple synthesis process, high efficiency, low preparation cost, reduced risk of contamination, and effective control over the resulting material's morphology. The structural characteristics were studied by X-ray diffractometer (XRD), the morphological features were monitored by Scanning Electron Microscopy (SEM), Energy Dispersive X-ray (EDX) spectroscopy and optical properties were examined by Ultraviolet–Visible (UV–vis) spectroscopy.

2. MATERIAL AND METHOD

Solid state reaction method was used to prepare the undoped ZnO and Sn-Al co-doped ZnO ($Zn_{1-x-y}Sn_xAl_yO$ ((x:y) = (0.00:0.00), (0.03:0.00), (0.00:0.03), (0.03:0.03)) samples. The stoichiometric amounts of starting powders ZnO, SnO_2 and Al_2O_3 were mixed and ground which is followed by calcination at 450 °C for 8 h. The resulting material was reground and pelletized upon cooling. Eventually, pellets of 10 mm diameter were prepared using press and these pellets were sintered at 900 °C for 12 h. The samples are referred as undoped ZnO (for x= 0, y= 0), Sn-ZnO (for x= 0.03, y= 0.00), Al-ZnO (for x= 0.00, y= 0.03) and (Sn, Al)-ZnO (for x= 0.03, y= 0.03).

For structural characterization, X-ray diffraction (XRD) using CuKα radiation (λ=1.5406 Å) accelerated in a 2θ range of 20–70° with a scan speed of 2° min^{-1} was performed. The surface morphology and grain structure of the samples were observed by scanning electron microscope (SEM) at magnification of 30 kx, and the elemental analysis of the samples was performed by energy-dispersive X-ray spectroscopy (EDX). The optical properties of all samples were characterized by using a UV–Vis spectrophotometer in the wavelength range of 300–800 nm.

3. RESULTS

3.1. XRD Analysis

Figure 1(a) demonstrates XRD patterns of undoped ZnO, $Zn_{0.97}Sn_{0.03}O$, $Zn_{0.97}Al_{0.03}O$ and $Zn_{0.94}Sn_{0.03}Al_{0.03}O$ samples. The diffraction patterns indexed with the 'hkl' values (100), (002), (101), (102), (110), (103), (200), (112) and (201) are the characteristic peaks of the hexagonal wurtzite crystal structure of ZnO (space group $P6_3mc$), which agrees with the standard data (JCPDS card No 36-1451).

An enlarged version of XRD pattern between 2θ= 31° and 37° to facilitate monitoring effect of doping on the structure is shown in Figure 1(b). The peaks (100), (002) and (101) of doped ZnO were slightly shifted to higher angles compared to undoped ZnO, which might have resulted from the compression of the lattice parameters due to the size difference between Sn, Al, and Zn atoms. The intensity of the peaks of doped ZnO decreased and the full width at half maximum (FWHM) became wider with doping. The lattice distortion produced around Sn and Al atoms increasing the tensile stress, may be held accountable for the decline in diffraction peak intensity and the increase of FWHM (Table 1).

Table 1. The peak position (2θ) values of undoped, Sn-doped, Al-doped and (Sn, Al) co-doped ZnO samples

Sample	(hkl)					
	(100)		(002)		(101)	
	2θ (°)	Intensity	2θ (°)	Intensity	2θ (°)	Intensity
ZnO	31.74	747	34.42	534	36.24	1376
Sn-ZnO	31.77	384	34.42	353	36.27	674
Al-ZnO	31.75	417	34.43	331	36.25	684
(Sn, Al)-ZnO	31.85	328	34.51	323	36.35	523

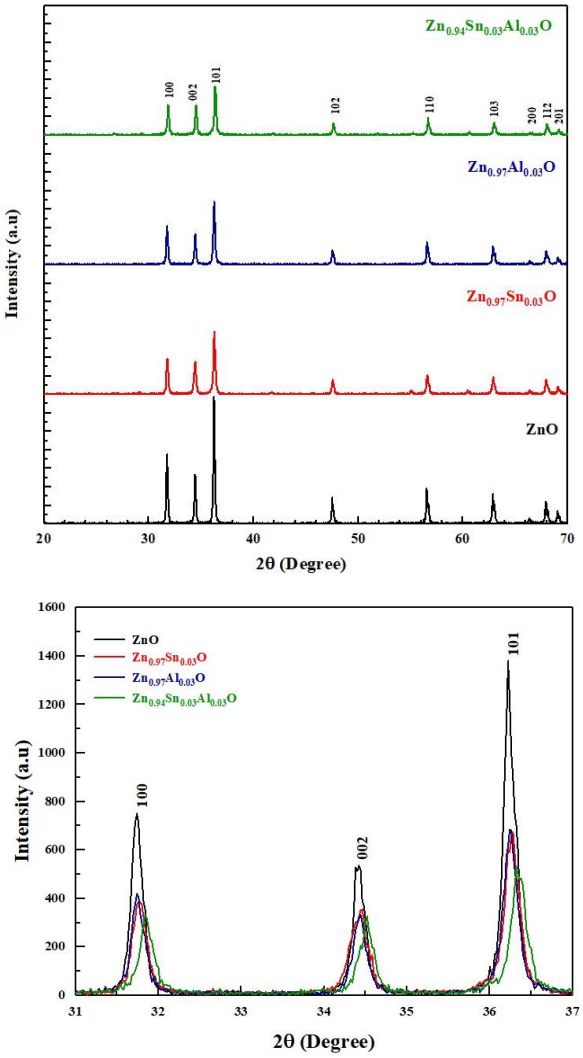

Figure 1. (a) XRD patterns of undoped ZnO, $Zn_{0.97}Sn_{0.03}O$, $Zn_{0.97}Al_{0.03}O$ and $Zn_{0.94}Sn_{0.03}Al_{0.03}O$ samples (b) enlarged view of (100), (002) and (101) peaks

Following relation was used to calculate the lattice constants (a, c) of the samples [45, 46]:

$$\frac{1}{d_{hkl}^2} = \frac{4}{3}\left(\frac{h^2 + hk + k^2}{a^2}\right) + \frac{l^2}{c^2} \quad (1)$$

where d_{hkl} is interplanar distance, determined from the Bragg's law ($2d_{hkl}\sin\theta = n\lambda$). From the lattice constants (a, c), the volume of the unit cell (V) for each sample was computed as follows [47, 48]:

$$V = \frac{\sqrt{3}}{2} a^2 c \quad (2)$$

The calculated values for the samples are given in table 2. The lattice parameters for undoped ZnO are a= 3.2523 Å, c= 5.2065 Å with unit cell volume V= 47.6920 Å^3. A small change was monitored in the lattice parameters a and c for Sn-ZnO compared to undoped ZnO which were prepared under same conditions. The lattice parameter a and c values decreased slightly after Al doping and Al, Sn co-doping. The radius of Al^{3+} (0.053 nm) and Sn^{4+} (0.069 nm) are smaller than the radius of Zn^{2+} (0.074 nm). In general, it is expected that the lattice constant gets smaller by Sn, Al atoms substituting Zn atoms in ZnO lattice. The lattice distortion c/a ratio is approximately 1.633 in a stoichiometric wurtzite structure. The calculated c/a of the samples are also given in table 2, and it was noticed that the values are slightly deviated from the ideal ratio indicating the presence of extended defects.

For hexagonal structure of ZnO, Zn–O bond length (L) was calculated via following equation [49, 50]:

$$L = \sqrt{\frac{a^2}{3} + \left(\frac{1}{2} - u\right)^2 c^2} \quad (3)$$

where u is a positional parameter of the wurtzite structure. The parameter u was calculated using below:

$$u = \frac{a^2}{3c^2} + 0.25 \quad (4)$$

The calculated value of Zn-O bond length (L) was found as 1.9788 Å for undoped ZnO, slightly higher than Zn-O bond length in the unit cell and decreased for doped ZnO. The bond length (L) and position parameter (u) values for the samples are listed in table 2.

Table 2. Lattice constants (a and c), unit cell volume (V), lattice distortion (c/a), displacement parameter (u) and bond length (L) of undoped, Sn-doped, Al-doped and (Sn, Al) co-doped ZnO samples

Sample	a(Å)	c(Å)	c/a	V (Å)^3	u	L (Å)
ZnO	3.2523	5.2065	1.6009	47.6920	0.3801	1.9788
Sn-ZnO	3.2493	5.2066	1.6024	47.6058	0.3798	1.8798
Al-ZnO	3.2514	5.2055	1.6010	47.6549	0.3800	1.8810
(Sn, Al)-ZnO	3.2412	5.1933	1.6023	47.2471	0.3798	1.8751

The crystallite size (D) and lattice strain (ε) were calculated using Scherrer's and Williamson–Hall method. The average crystallite size (D) was calculated below using Scherrer's equation [51, 52]:

$$D = \frac{K\lambda}{\beta cos\theta} \quad (5)$$

where K is the shape factor (is approximately given as 0.9), λ is the wavelength of Cu-K_α radiation (λ= 0.15406 nm), and β is full width at half maximum (FWHM). For undoped, Sn-doped, Al-doped and (Sn, Al) co-doped ZnO samples, average crystallite size was calculated as 35.69, 32.63, 33.06 and 30.10 nm, respectively. The average crystallite size of the samples was smaller than that of undoped ZnO as shown in table 3. The decrease in the crystallite size might be due to the distortion in the host ZnO lattice.

The lattice strain (ε) values were calculated using the following formula [53]:

$$\varepsilon = \frac{\beta cot\theta}{4} \quad (6)$$

The calculated lattice strain (ε) values are given in table 3. It was clearly seen that in doped samples average crystallite size (D) decreases while lattice strain values (ε) increases compared to undoped ZnO. To approximate structural flaws in the samples, dislocation density (δ) is an important parameter. Following equation gives the dislocation density (δ) [54, 55]:

$$\delta = \frac{1}{D^2} \quad (7)$$

The dislocation density variation trend is like that of lattice strain, which is the expected behavior. It was observed that diffraction broadening causes a decrease in crystallite size (D) and an increase in lattice strain (ε). This may be attributed to the growth in the overall defect concentration in the structure.

W-H method yields a more accurate crystallite size than that of obtained using Scherrer's method, as W–H method considers the contribution of intrinsic strain due to i.e. the presence of point defect, stacking faults, grain boundaries. The average crystallite size (D) and strain (ε) were determined below using Williamson-Hall method [56, 57]:

$$\beta cos\theta = \frac{K\lambda}{D} + 4\varepsilon sin\theta \quad (8)$$

The plots of βcosθ as a function of 4sinθ for all samples are shown in figure 2. The y-intercept of the corresponding linear fit extrapolation is used to determine D values, while the slope of this fit gives ε values. The strain and crystallite size values obtained from W-H plot is given in table 3.

The calculated value of D and ε for undoped ZnO by Scherrer's method is 35.69 nm and 2.42x10^{-3}, respectively. By Williamson–Hall's method, D is found as 118.50 nm which is larger than that obtained by Scherrer's method, while ε is smaller, which is 1.68x10^{-3}. The reduction in the ε may explain the strain contribution in crystal size using Williamson–Hall's method that leads to obtaining large size compared to Scherrer's method. In both method, D decreased with doping Sn and Al into ZnO, which may be attributed to the slight decrease in the lattice parameters.

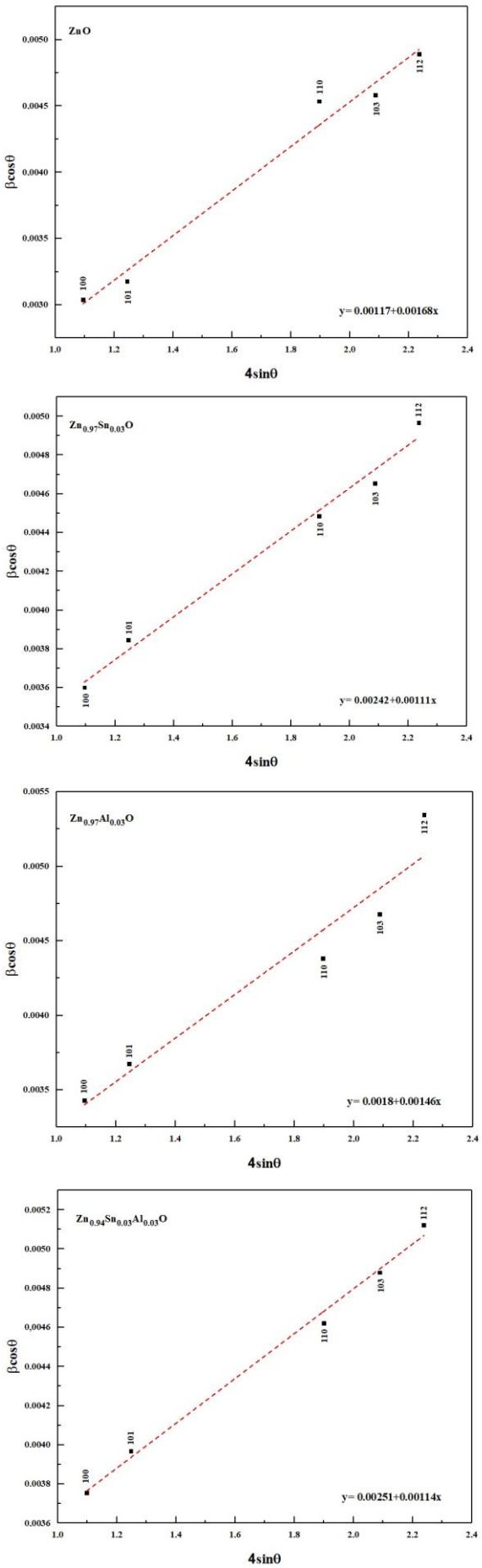

Figure 2. βcosθ versus 4sinθ of undoped ZnO, $Zn_{0.97}Sn_{0.03}O$, $Zn_{0.97}Al_{0.03}O$ and $Zn_{0.94}Sn_{0.03}Al_{0.03}O$ samples

Table 3. The calculated crystallite size (D), dislocation density (δ) and the lattice strain (ε) for undoped, Sn-doped, Al-doped and (Sn, Al) co-doped ZnO samples

Sample	Scherrer's D (nm)	ε (10^{-3})	δ $(nm)^{-2}$	W-H	
				D (nm)	ε (10^{-3})
ZnO	35.69	2.42	0.00078	118.50	1.68
Sn-ZnO	32.63	2.64	0.00094	57.29	1.11
Al-ZnO	33.06	2.61	0.00091	77.03	1.46
(Sn, Al)-ZnO	30.10	2.56	0.00110	55.24	1.14

3.2. SEM and EDX Analysis

SEM images of undoped ZnO and co-doped ZnO are displayed in figure 3. In all samples, it was monitored that the grains were homogeneously distributed and there were hexagonal like grains. Grains were more closely packed in undoped sample, whereas the voids between the grains increased with doping which may be linked to the existence of defects. SEM images also showed that the grain size was smaller in doped samples when compared to the undoped ZnO. In accordance with the crystallite size obtained from XRD measurements, it was observed from SEM images that the grain sizes decreased with doping.

Figure 4 presents the EDX spectra of all samples. Each image includes an inset showing the atomic and molecular weights of the elements involved in the synthesis process. It was observed that all the samples contain Zn, Sn, Al, and O elements according to their respective stoichiometric amounts. EDX spectrum and elemental mapping confirmed the presence of the host and substituted elements without any other element. The dopant concentration and reduction in host element content indicated that materials retain their stoichiometric compositions.

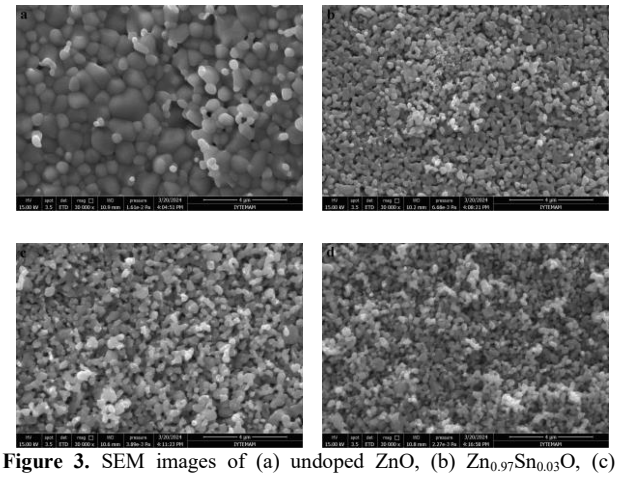

Figure 3. SEM images of (a) undoped ZnO, (b) $Zn_{0.97}Sn_{0.03}O$, (c) $Zn_{0.97}Al_{0.03}O$ and (d) $Zn_{0.94}Sn_{0.03}Al_{0.03}O$ samples at 30000×magnifcation

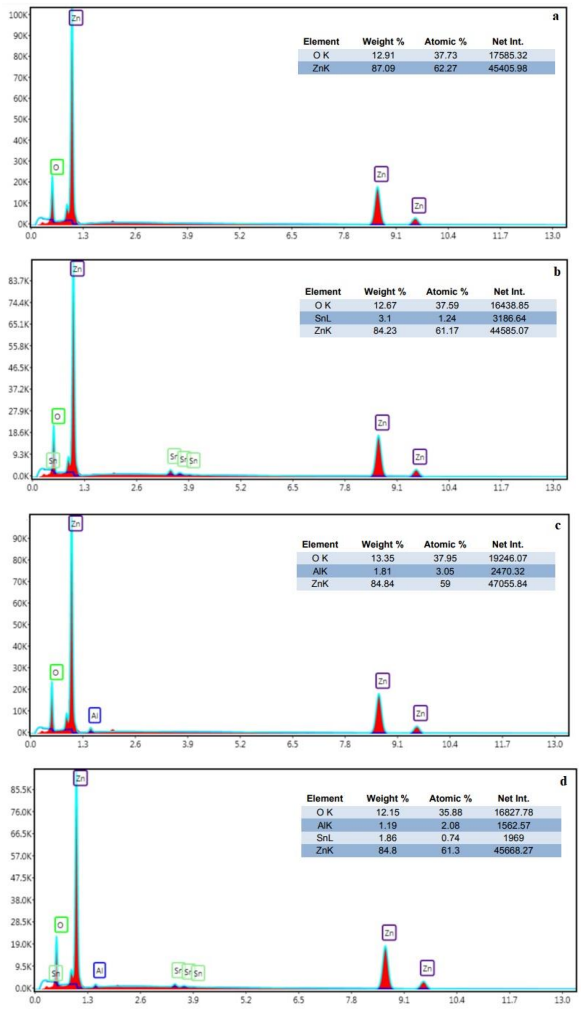

Figure 4. EDX spectra of (a) undoped ZnO, (b) $Zn_{0.97}Sn_{0.03}O$, (c) $Zn_{0.97}Al_{0.03}O$ and (d) $Zn_{0.94}S_{n0.03}Al_{0.03}O$ samples

3.3. UV–Vis Spectroscopy Analysis

The impact of doping on the optical properties of ZnO was investigated via reflectance UV–vis spectroscopy measurement in the wavelength range of 300−800 nm. Reflectance spectra of undoped and doped ZnO are displayed in figure 5. From the reflectance spectra, the absorption edge spectra for each sample were determined. The reflectance data was converted to absorption spectra through Kubelka-Munk equation. The optical absorption spectra of all samples are displayed in figure 6. The absorption edge spectra of doped samples were shifted towards higher wavelength as compared to undoped ZnO sample.

Tauc equation was used to calculate the optical band gap energy (E_g) [58, 59]:

$$\alpha h\upsilon = A\left(h\upsilon - E_g\right)^n \quad (9)$$

where α is the absorption coefficient ($\alpha = 2.303A/t$) and n is a constant depending on optical transition type and equal to 1/2 for direct gap transitions. Figure 7 denotes the plotting of $(\alpha h\upsilon)^2$ as a function of photon energy hυ. Plotting a line tangent to the linear part of the $(\alpha h\upsilon)^2$ versus hν curve and taking its intersection point with the x-axis (hν) gives the energy bandgap, E_g. The obtained results are also listed in table 4.

The energy band gap value of the prepared undoped ZnO was estimated as 3.27 eV which is less than that the reported for ZnO (3.37 eV). This deviation might be driven by the structural defects that encompass the sample during the synthesis process and thermal treatment. A slight decrease compared to undoped ZnO was observed with doping and co-doping. The samples' estimated band gap values were retrieved as 3.26, 3.23 and 3.25 eV for $Zn_{0.97}Sn_{0.03}O$, $Zn_{0.97}Al_{0.03}O$ and $Zn_{0.94}Sn_{0.03}Al_{0.03}O$, respectively. Compared with that of Sn doping, it was seen that Al doping makes the band gap narrowing more apparent. The values being close to each other may be attributed to low doping concentration.

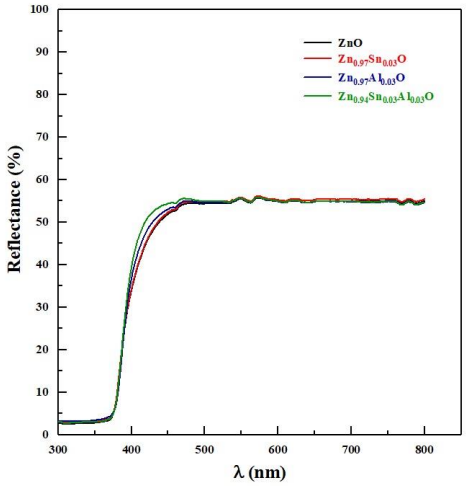

Figure 5. Reflectance spectra of undoped ZnO, $Zn_{0.97}Sn_{0.03}O$, $Zn_{0.97}Al_{0.03}O$ and $Zn_{0.94}Sn_{0.03}Al_{0.03}O$ samples

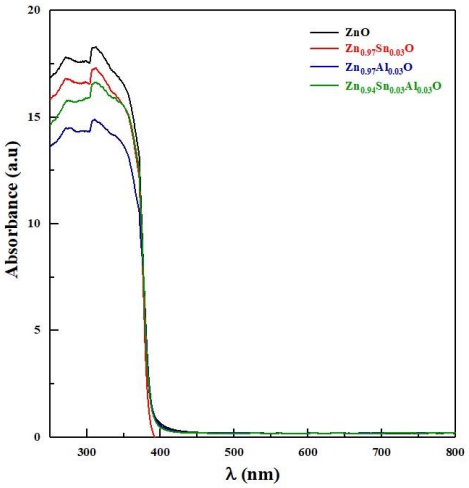

Figure 6. Absorbance spectra of undoped ZnO, $Zn_{0.97}Sn_{0.03}O$, $Zn_{0.97}Al_{0.03}O$ and $Zn_{0.94}Sn_{0.03}Al_{0.03}O$ samples

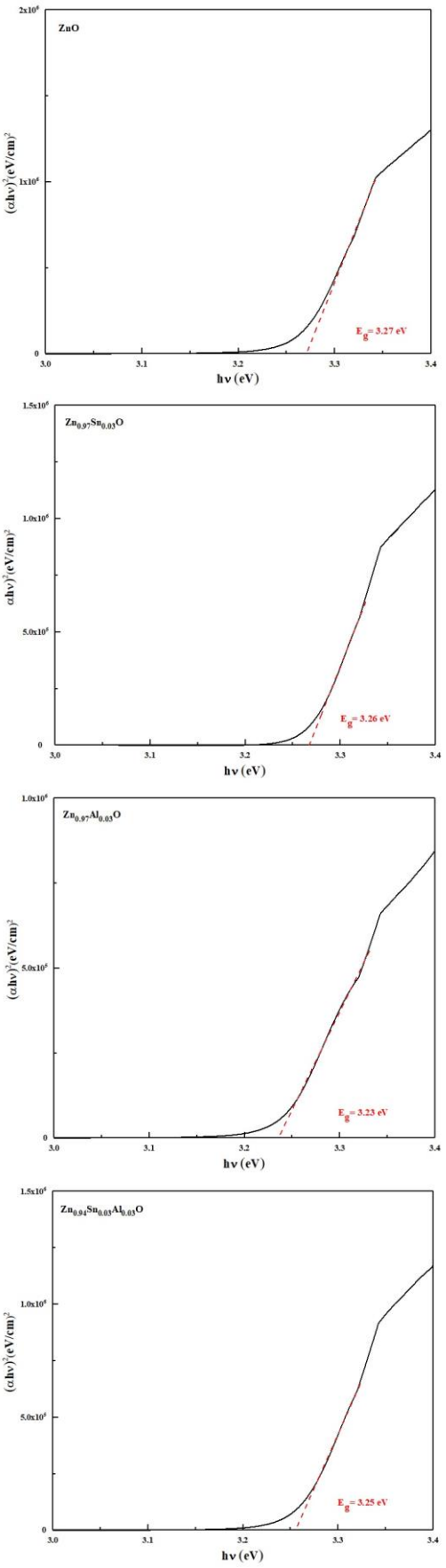

Figure 7. Tauc plots of undoped ZnO, $Zn_{0.97}Sn_{0.03}O$, $Zn_{0.97}Al_{0.03}O$ and $Zn_{0.94}Sn_{0.03}Al_{0.03}O$ samples

The band gap of ZnO exhibits a slight reduction upon doping with Al and Sn, which is attributed to the presence of defect bands in the band gap. Interactions between ZnO lattice and dopant ions leads to the creation of localized states within ZnO band gap. An urbach tail is produced by these defect states which extends deep into the forbidden gap and the energy associated with this tail is referred as Urbach energy [60].

The Urbach energy (E_u), which correlates the band tails of the localized states with the crystal defects and microstructural lattice disorders, and is determined from the following relation [61-63]:

$$\alpha = \alpha_0 \exp\left(h\nu/E_u\right) \quad (10)$$

where α_0 is a constant, α is the absorption coefficient, and hν is the photon energy. E_u is determined by plotting ln(α) versus (hν). The value of E_u was obtained by taking the reciprocal of the slope of the linear fit. The obtained values of E_u are given in table 4.

The values of Urbach energy evaluated from the slopes of the fitted curves were found as 0.491, 0.554, 0.577 and 0.660 eV for undoped ZnO, $Zn_{0.97}Sn_{0.03}O$, $Zn_{0.97}Al_{0.03}O$ and $Zn_{0.94}Sn_{0.03}Al_{0.03}O$, respectively. An opposite trend in the variations of E_u and E_g with doping concentration was observed. The E_u value is relatively high for doped samples, and this might be associated with structural defects or disorder presents in the samples.

The Urbach energy of doped ZnO was found to be higher than that of undoped ZnO. Previous studies have reported that increasing Urbach energy results in an increase in dislocation density. Consistent with the XRD and UV–vis spectroscopy results, the observed increase in Urbach energy in doped ZnO was accompanied by an increase in dislocation density [64-65].

Table 4. The optical band gap (E_g) and Urbach (E_u) energy for undoped, Sn-doped, Al-doped and (Sn, Al) co-doped ZnO samples

Sample	E_g (eV)	E_u (eV)
ZnO	3.27	0.491
Sn-ZnO	3.26	0.554
Al-ZnO	3.23	0.577
(Sn, Al)-ZnO	3.25	0.660

4. DISCUSSION AND CONCLUSION

The effects of Al, Sn doping and co-doping on the structural, optical, and morphological properties of ZnO samples prepared by solid-state reaction method were reported in this study. XRD, SEM, EDX, and U-Vis measurements were deployed to investigate the main characteristic features of the samples. From XRD, it was concluded that the doping resulted with no change in the hexagonal wurtzite structure of ZnO. With doping, there was a slight decrease in the cell parameters and bond length which results in the shrink of the cell volume. The crystallite size (D) estimated both by Scherrer's and Williamson–Hall methods decreased with Sn, Al doping and with (Sn-Al) co-doping compared to undoped ZnO. SEM indicated the presence of hexagonal like grains in all samples and showed that the grain size decreases with doping. The band gap values were determined to be 3.26 eV and 3.23 eV for Sn and Al-doped ZnO, respectively,

and 3.25 eV for Sn, Al co-doped ZnO, compared to 3.27 eV for undoped ZnO. According to the UV–Vis spectroscopy data, both doping and co-doping of ZnO led to a slight narrowing of the band gap and an increase in Urbach energy compared to undoped ZnO. The increase in Urbach energy may be attributed to a higher degree of structural disorder and a reduction in crystallite size resulting from the incorporation of Al and Sn dopants into the ZnO lattice. Overall, the obtained results suggested that the structural and optical properties of ZnO can be altered by doping.

Acknowledgement

Samples were prepared at Physics Laboratory Dokuz Eylul University, Faculty of Science, Physics Department, in Izmir, Turkey. XRD and U-Vis measurements were performed at Electronic Materials Production and Application Center (EMUM) Dokuz Eylul University. SEM and EDX were performed at İzmir Institute of Technology Integrated Research Centers.

REFERENCES

[1] Boshra Ghanbari Shohany, Ali Khorsand Zak. Doped ZnO nanostructures with selected elements - Structural, morphology and optical properties: A review, Ceramics International 2020; 46: 5507-5520.

[2] Dhirendra Kumar Sharma, Sweta Shukla, Kapil Kumar Sharma, Vipin Kumar. A review on ZnO: Fundamental properties and applications, Materials Today: Proceedings. 2022; 49: 3028-3035.

[3] Dongwoon Jung. Syntheses and characterizations of transition metal-doped ZnO, Solid State Sciences 2010; 12: 466-470.

[4] Asikuzun Tokeser E., Ozturk O. . Estimation of microstructural parameters by Williamson–Hall, Halder–Wagner, and size–strain plot methods and magnetic properties of (Cu/Mn) co-doped ZnO nanoparticles, J Mater Sci: Mater Electron. 2023; 34: 2075

[5] Geetha Devi P., Sakthi Velu A.. Synthesis, structural and optical properties of pure ZnO and Co doped ZnO nanoparticles prepared by the co-precipitation method. J Theor Appl Phys. 2016; 10: 233–240.

[6] Xiurong Qu, Shuchen Lu, Dechang Jia, Sheng Zhou, Qingyu Meng. First-principles study of the electronic structure of Al and Sn co-doping ZnO system, Materials Science in Semiconductor Processing 2013; 16: 1057-1062.

[7] Huaming Yang, Sha Nie. Preparation and characterization of Co-doped ZnO nanomaterials. Materials Chemistry and Physics 2009; 114: 279–282.

[8] Amalia M., Cristina D. G, Mihaela P., Raluca M, Adriana Popa, Traian Petrisor Jr., Mihai Gabor, Adrian Ionut Cadis, Bogdan S. Vasile. Synthesis, structural and morphological characteristics, magnetic and optical properties of Co doped ZnO nanoparticles, Ceramics International 2014; 40: 2835-2846.

[9] Chao Xu, Lixin Cao, Ge Su, Wei Liu, Xiaofei Qu, Yaqin Yu, Preparation, characterization and photocatalytic activity of Co-doped ZnO powders, Journal of Alloys and Compounds 2010; 497: 373–376.

[10] N.H. Erdogan, T. Kutlu, N. Sedefoglu, H. Kavak Effect of Na doping on microstructures, optical and electrical properties of ZnO thin films grown by sol-gel method. Journal of Alloys and Compounds 2021; 881: 160554.

[11] Imen Massoudi, Taher Ghrıb, Amal L. Al-Otaıbı, Kawther Al-Hamadah, Shadıa Al-Malky, Maha Al-Otaıbı, and Marıam Al-Yatımı Effect of Yttrium Substitution on Microstructural, Optical, and Photocatalytic Properties of ZnO Nanostructures, Journal of Electronic Materials 2020; 49: 5353-5362.

[12] G. Murtaza, R. Ahmad, M.S. Rashid, M. Hassan, A. Hussnain, Muhammad Azhar Khan, M. Ehsan ul Haq, M.A. Shafique, S. Riaz Structural and magnetic studies on Zr doped ZnO diluted magnetic semiconductor, Current Applied Physics 2014; 14: 176-181.

[13] R. Elilarassi, G. Chandrasekaran Structural, optical and magnetic characterization of Cu-doped ZnO nanoparticles synthesized using solid state reaction method, J Mater Sci: Mater Electron. 2010; 21: 1168–1173.

[14] Zafer Gultekin, Mursel Alper1, M. Cuneyt Hacıismailoglu, and Cengiz Akay Effect of Mn doping on structural, optical and magnetic properties of ZnO films fabricated by sol–gel spin coating method, J Mater Sci: Mater Electron. 2023; 34: 2-14.

[15] G. Bulun, A. Ekicibil, S. K. Cetin, S. Demirdis, A. Coskun, K. Kıymac Elaboration of the structural and physical characteristics: Ni-doped ZnO bulk samples prepared by solid state reactions, Journal of Optoelectronics and Advanced Materials 2011; 13: 231-236.

[16] Sujit Anil Kadam, Susmi Anna Thomas, Yuan-Ron Ma, Lolly Maria Jose, D. Sajan, Arun Aravind Investigation of adsorption and photocatalytic behavior of manganese doped zinc oxide nanostructures, Inorganic Chemistry Communications 2021; 134: 108981.

[17] T. Akilan, N. Srinivasan, R. Saravanan Magnetic and optical properties of Ti doped ZnO prepared by solid state reaction method, Materials Science in Semiconductor Processing 2015; 30: 381-387.

[18] Jing Xie, Yali Cao, Dianzeng Jia, Yizhao Li, Yang Wang Solid-state synthesis of Y-doped ZnO nanoparticles with selective-detection gas-sensing performance Ceramics International 2016; 42: 90-96.

[19] Hakan Colak, Orhan Turkoglu Structural and electrical properties of V-doped ZnO prepared by the solid-state reaction, J Mater Sci: Mater Electron. 2012; 23: 1750–1758.

[20] N. K. Divya, P.P. Pradyumnan, Solid state synthesis of erbium doped ZnO with excellent photocatalytic activity and enhanced visible light emission, Materials Science in Semiconductor Processing 2016; 41: 428-435.

[21] Chaeseon Hong, Kyung-Mun Kang, Minjae Kim, Yue Wang, Taehee Kim, Chan Lee, Hyung-Ho Park Structural, electrical, and optical properties of Si-doped ZnO thin films prepared via supercycled atomic layer deposition, Materials Science and Engineering: B 2021; 273: 115401.

[22] Caiying Mao, Liang Fang, Hong Zhang, Wanjun Li, Fang Wu, Guoping Qin, Haibo Ruan, Chunyang Kong Effect of B doping on optical, electrical properties and defects of ZnO films, Journal of Alloys and Compounds 2016; 676: 135-141.

[23] Bircan Dindara, Ali Can Güler Comparison of facile synthesized N doped, B doped and undoped ZnO for the photocatalytic removal of Rhodamine B. Environmental Nanotechnology, Monitoring & Management 2018; 10: 457-466

[24] J. Mayandi, R.K. Madathil, C. Abinaya, K. Bethke, V. Venkatachalapathy, K. Rademann, T. Norby, T.G. Finstad Al-doped ZnO prepared by co-precipitation method and its thermoelectric characteristics, Materials Letters 2021; 288: 129352.

[25] Chien-Yie Tsay, Hua-Chi Cheng, Yen-Ting Tung, Wei-Hsing Tuan, Chung-Kwei Lin Effect of Sn-doped on microstructural and optical properties of ZnO thin films deposited by sol–gel method Thin Solid Films 2008; 517: 1032–1036.

[26] Rajwali Khan, Vineet Tirth, Amjad Ali Kashif Irshad, Nasir Rahman, Ali Algahtani, Mohammad Sohail, Saiful Isalm Effect of Sn-doping on the structural, optical, dielectric and magnetic properties of ZnO nanoparticles for spintronics applications, J Mater Sci: Mater Electron. 2021; 32: 21631–2164.

[27] A.D. Acharya, Shweta Moghe, Richa Panda, S.B. Shrivastava, Mohan Gangrade, T. Shripathi, D.M. Phase, V. Ganesan Growth and characterization of nano-structured Sn doped ZnO, Journal of Molecular Structure 2012; 1022 8-15.

[28] Manjeet Kumar, Vishwa Bhatt, A.C. Abhyankar, Joondong Kim, Akshay Kumar, Ju-Hyung Yun Modulation of structural properties of Sn doped ZnO for UV photoconductors, Sensors and Actuators A: Physical 2018; 270: 118-126.

[29] Mustafa Ozgür, Suat Pat, Reza Mohammadigharehbagh, Caner Musaoglu, Ugur Demirkol, Saliha Elmas, Soner Ozen, Sadan Korkmaz Sn doped ZnO thin film deposition using thermionic vacuum arc technique, Journal of Alloys and Compounds 2019; 774: 1017-1023.

[30] Mejda Ajili, Michel Castagné, Najoua Kamoun Turki Study on the doping effect of Sn-doped ZnO thin films, Superlattices and Microstructures 2013; 53: 213-222.

[31] H. Aydin, H.M. El-Nasser, C. Aydin, Ahmed. A. Al-Ghamdi, F. Yakuphanoglu Synthesis and characterization of nanostructured undoped and Sn-doped ZnO thin films via sol–gel approach, Applied Surface Science 2015; 350: 109-114.

[32] Weibao Guan, Liying Zhang, Chao Wang, Yuanxu Wang Theoretical and experimental investigations of the thermoelectric properties of Al-, Bi- and Sn-doped ZnO, Materials Science in Semiconductor Processing 2017; 66: 247-252.

[33] Jin Zhaoa, Qiao Liping, Guo Chen, He Zhili, Liu Lidong, Rong Mei First-priniciple study of electrical and optical properties of (Al,Sn) co-doped ZnO, Optik 2016; 127: 1988-1992.

[34] Susanta Kumar Sahoo, Chandan Ashis Gupta, Udai P. Singh Impact of Al and Ga co-doping with different proportion in ZnO thin film by DC magnetron sputtering, J Mater Sci: Mater Electron. 2016; 27: 7161–7166.

[35] M. K. Alqadi, A. B. Migdadi, F. Y. Alzoubi, H. M. Al-Khateeb, Ahmad A. Almasri, Influence of (Ag–Cu) co-doping on the optical, structural, electrical, and morphological properties of ZnO thin films, Journal of Sol-Gel Science and Technology 2022; 103: 319–334.

[36] G. Vijayaprasath, R. Murugan, S. Asaithambi, P. Sakthivel, T. Mahalingam, Y. Hayakawa, G. Ravi Structural and magnetic behavior of Ni/Mn co-doped ZnO nanoparticles prepared by co-precipitation method, Ceramics International 2016; 42: 2836–2845.

[37] Rajwali Khan, Simbarashe Fashu, Zia-Ur-Rehman Structural, dielectric and magnetic properties of (Al, Ni) co-doped ZnO nanoparticles, J Mater Sci: Mater Electron. 2017; 28: 4333–4339.

[38] B. Poornaprakash, U. Chalapathi, S. Babu, Si-Hyun Parka Structural, morphological, optical, and magnetic properties of Gd-doped and (Gd, Mn) co-doped ZnO nanoparticles, Physica E: Low-dimensional Systems and Nanostructures 2017; 93: 111-115.

[39] Wubishet Kejela Tolossa, Paulos Taddesse Shibeshi Structural, optical and enhanced antibacterial activities of ZnO and (Co, Fe) co-doped ZnO nanoparticles by sol-gel combustion method, Chemical Physics Letters 2022; 795: 139519.

[40] Fazal Kabir, Adil Murtaza, Azhar Saeed, Awais Ghani, Anwar Ali, Saleh Khan, Kaili Li, Qizhong Zhao, Kang Kang Yao, Yin Zhang, Sen Yang Structural, optical and magnetic behavior of (Pr, Fe) co-doped ZnO based dilute magnetic semiconducting nanocrystals, Ceramics International 2022; 48: 19606-19617.

[41] Rajwali Khan, Zulfiqar, Simbarashe Fashu, Zia Ur Rehman, Aurangzeb Khan, Muneeb Ur Rahman Structure and magnetic properties of (Co, Mn) co-doped ZnO diluted magnetic semiconductor nanoparticles, J Mater Sci: Mater Electron. 2018; 29: 32–37.

[42] Sudipta Mondal, Moniruzzaman Jamal, Sikder Ashikuzzaman Ayon, Md Jannatul Ferdous Anik, Md Muktadir Billah Synergistic enhancement of photocatalytic and antimicrobial efficacy of nitrogen and erbium co-doped ZnO nanoparticles, Journal of Rare Earths 2024; 42: 859-868.

[43] S.D. Senol, E. Ozugurlu, L. Arda Synthesis, structure and optical properties of (Mn/Cu) co-doped ZnO nanoparticles, Journal of Alloys and Compounds 2020; 822: 153514.

[44] Darshan Sharma, Ranjana Jha Transition metal (Co, Mn) co-doped ZnO nanoparticles: Effect on

structural and optical properties, Journal of Alloys and Compounds 2017; 698: 532-538
[45] Anu Katiyar, Nishant Kumar, Priyanka Srivastava, R.K. Shukla, Anchal Srivastava Structural and physical parameters of sol-gel spin coated ZnO thin films: Effect of sol concentration, Materials Today: Proceeding 2020; 29: 1098-1103.
[46] Esra Aslan, Maharram Zarbali Tuning of photosensitivity and optical parameters of ZnO based photodetectors by co-Sn and Ti doping, Optical Materials 2022; 125: 112030.
[47] Mona A. Mohaseb Effect of Co doping onto physical properties of ZnO films and its UV detection performance, J Mater Sci: Mater Electron. 2023; 34: 1219.
[48] A. Khorsand Zak, W.H. Abd. Majid, M.E. Abrishami, Ramin Yousefi X-ray analysis of ZnO nanoparticles by Williamson-Hall and size estrain plot methods, Solid State Sciences 2011; 13: 251-256.
[49] H. Saadia, F.I.H. Rhouma, Z. Benzarti, Z. Bougrioua, S. Guermazi, K. Khirouni Electrical conductivity improvement of Fe doped ZnO nanopowders, Materials Research Bulletin 2020; 129: 110884.
[50] A. A. Ahmad, A. B. Migdadi, A. M. Alsaad, Qais M. Al-Bataineh, Ahmad Telfah Optical, structural, and morphological characterizations of synthesized (Cd–Ni) co-doped ZnO thin flms, Applied Physics A 2021; 127: 922.
[51] Noubeil Guermat, Warda Daranfed, Idris Bouchama, Nadir Bouarissa Investigation of structural, morphological, optical and electrical properties of Co/Ni co-doped ZnO thin films, Journal of Molecular Structure 2021; 1225: 129134
[52] N. Siva, D. Sakthi, S. Ragupathy, V. Arun, N. Kannadasan Synthesis, structural, optical and photocatalytic behavior of Sn doped ZnO nanoparticles, Materials Science and Engineering: B 2020; 253: 114497.
[53] Aradhana Tiwari, P.P. Sahay Highly c-axis oriented (Mg, Sn) co-doped ZnO thin films for optoelectronic applications, Optical Materials 2022; 134: 113098.
[54] Safa Hamdi, Hichem Smaoui, Samir Guermazi, Gerard Leroy, Benoit Duponchel Enhancing the structural, optical and electrical conductivity properties of ZnO nanopowders through Dy doping, Inorganic Chemistry Communications 2022; 144: 109819.
[55] V. Ganesh, I.S. Yahia, S. AlFaify, Mohd. Shkir Sn-doped ZnO nanocrystalline thin films with enhanced linear and nonlinear optical properties for optoelectronic applications, Journal of Physics and Chemistry of Solids 2017; 100: 115-125.
[56] P. Norouzzadeh, Kh. Mabhouti, M. M. Golzan, R. Naderali Consequence of Mn and Ni doping on structural, optical and magnetic characteristics of ZnO nanopowders: the Williamson–Hall method, the Kramers–Kronig approach and magnetic interactions, Applied Physics A 2020; 126: 154
[57] Shradha Roy, Mritunjoy Prasad Ghosh, Samrat Mukherjee Introducing magnetic properties in Fe-doped ZnO nanoparticles, Applied Physics A 2021; 127: 451
[58] T. Ates, C. Tatar, F. Yakuphanoglu Preparation of semiconductor ZnO powders by sol–gel method: Humidity sensors, Sensors and Actuators A: Physical 2013; 190: 153-160.
[59] Yongmei Zhu, Guoyue Xu, Tengchao Guo, Haili Hou, Shujuan Tan Preparation, infrared emissivity and thermochromic properties of Co doped ZnO by solid state reaction, Journal of Alloys and Compounds 2017; 720: 105-115.
[60] Cosmas Muiva, Dineo P. Sebuso, Edigar Muchuweni, Microstructural and optical properties of nanostructured Al/Ag co-doped ZnO thin films (AgxAl0.03ZnO0.97-x) by spray pyrolysis for optoelectronic applications, Physica B 2024; 690: 416206.
[61] S. Rajasekar, Jafar Ali Ibrahim Syed Masood, N.S. Kalyan Chakravarthi, P. Shunmuga Sundaram, M. Karunakaran, Gaurav Jayaswal, L. Bruno Chandrasekarf, Abdullah N. Alodhayb, George Z. Kyzas, Synthesis and characterization of cobalt-strontium co-doped zinc oxide nanoparticles by chemical precipitation, Inorganic Chemistry Communications 2023; 158: 111607.
[62] Mehmet Ozkan, Sercan Sadık Erdem, Reza Mohammadigharehbagh, Sema Kurtaran, Suat Pat Investigation of substrate effect on Co-doped ZnO thin films prepared by thermionic vacuum arc technique, Inorganic Chemistry Communications 2022; 146: 110095.
[63] M. Thobega, K. Maabong-Tau, K. Lefatshe, C. Muiva, Study of structural, optical and electrical properties of Nickel doped ZnO (Ni–ZnO) nanorods grown by chemical bath deposition, Physica B 2024; 673: 415500.
[64] K. Salima, M. Medles, A. Nakrela, R. Miloua, A. Bouzidi, R. Desfeux, Enhancement of optical and electrical properties of spray pyrolysed ZnO thin films obtained from nitrate chemical by Al-Sn co-doping, Optik 2020; 210: 164504.
[65] Imadeddine Bellili, Mohamed Mahtali, Warda Darenfad, Noubeil Guermat, The figure of merit improvement of (Sn, Co)–ZnO sprayed thin films for optoelectronic applications, Optical Materials 2024;154: 115785.